

# Patterns of shift in ADC distributions in abdominal tumours during chemotherapy—feasibility study

Kirsteen McDonald · Neil J. Sebire · John Anderson · Øystein E. Olsen

Received: 22 January 2010 / Revised: 9 May 2010 / Accepted: 10 May 2010 / Published online: 2 July 2010  
© Springer-Verlag 2010

## Abstract

**Background** Apparent diffusion coefficient (ADC) relates to tissue cellularity, and change in ADC during chemotherapy may be a promising tool for assessing oncological response.

**Objective** To investigate the feasibility of measuring changes in ADC distribution in solid abdominal and pelvic paediatric tumours during chemotherapy, and to assess patterns of change.

**Materials and methods** Consecutive children were included in a prospective observational study. ADC maps were calculated at presentation and following chemotherapy from a diffusion-sensitised sequence. ADC distribution in the whole tumour, excluding areas of low or absent gadolinium-enhancement, was investigated. Change during chemotherapy was assessed for each patient individually. Histopathological slices from the resected specimens were reviewed.

**Results** There were seven children (nine tumours) included in the study. ADC in all except one deviated from a normal distribution. All tumours changed their ADC distribution

during chemotherapy. Median ADC increased in all upper abdominal tumours, but more in tumours with histopathologically good or marked response to chemotherapy. Seven out of nine tumours attained a wider ADC distribution, the remaining two showed little chemotherapy response.

**Conclusion** ADC distribution changes during chemotherapy in childhood abdominal tumours are measurable. Distinct patterns of shift can be observed and ADC change is therefore promising as a noninvasive biomarker for therapy response.

**Keywords** Neoplasm · Therapy assessment · MRI · Diffusion-weighted imaging · Child

## Introduction

Assessment of chemotherapy response in solid tumours has traditionally been based on changes in tumour size on cross-sectional imaging, but this is often a late marker, which is unreliable in the presence of substantial necrosis. Further, tissue differentiation may be seen despite an increase in volume. Conversely, tumours that shrink substantially may still be composed predominantly of malignant cells [1, 2]. New noninvasive imaging biomarkers are therefore needed.

There is a relationship between histopathological tumour cellularity and apparent diffusion coefficient (ADC) as highly cellular tumours have lower ADC values and less cellular tumours have higher ADC [3]. Chemotherapy response at tissue level is seen as tumour cell necrosis and replacement by macrophages and fibroblasts. Since such decreases in tumour cellularity are histopathological expressions of chemotherapy response, we hypothesised that a corresponding shift in ADC distributions towards higher

K. McDonald · Ø. E. Olsen (✉)  
Radiology Department,  
Great Ormond Street Hospital for Children NHS Trust,  
Great Ormond Street,  
London WC1N 3JH, UK  
e-mail: olseno@gosh.nhs.uk

N. J. Sebire  
Histopathology Department,  
Great Ormond Street Hospital for Children NHS Trust,  
London, UK

J. Anderson  
Oncology Department,  
Great Ormond Street Hospital for Children NHS Trust,  
London, UK

values over the course of chemotherapy may be measurable by diffusion-weighted MRI (DWI). If so, ADC might be a useful noninvasive biomarker for therapy response.

The purpose of this prospective observational study was to investigate the feasibility of identifying differences in ADC distributions in the entire viable portion(s) of primary solid abdominal and pelvic childhood tumours before and after chemotherapy, and to explore the patterns of any such shifts.

## Materials and methods

Ethical approval for this study was obtained from the research ethics committee of our institution.

Data collection was performed prospectively in consecutive children who were referred for routine protocol-driven MRI assessment of primary abdominal and pelvic solid tumours in a tertiary paediatric hospital between July 2007 and December 2008. Our institution generally prefers MRI over CT; however, due to capacity issues not all patients will have MRI both at primary diagnosis and at post-chemotherapy follow-up. Only those who had MR imaging both before treatment and following chemotherapy were included in this study. The interval between the first and second scans was determined by the relevant oncological treatment protocol. Exclusion criteria were: any oncological treatment (chemotherapy or radiotherapy) before initial imaging, specimen unavailable for histopathological assessment and tumours where the largest area on a single slice was  $<3 \text{ cm}^2$  on any single scan.

Children were awake, sedated or under general anaesthesia for the scan depending on their ability to cooperate and depending on an anaesthesiological safety assessment that adhered to local policy [4]. All had peripheral or central venous access. To attenuate peristaltic artefact, 0.4 mg/kg body weight of hyoscine butylbromide (Buscopan, Boehringer Ingelheim Limited, Bracknell, UK) was given intravenously at the start of the scan. Gadoteric acid (Dotarem, Guerbet, Roissy, France) was used in all children at an intravenous dose of 0.05 mmol/kg body weight. All children were screened for risk factors for nephrogenic systemic fibrosis before the scan. This included estimation of glomerular filtration rate in all children post chemotherapy and in all children with a history or a suspicion of renal disease. There were no complications to the sedation, anaesthetic procedure, diagnostic drugs or the scanning.

### MRI acquisitions

MRI was performed on one of two Siemens Magnetom Avanto (Siemens, Erlangen, Germany) 1.5-T MRI scanners. Coil selection depended on body size, with a preference for

the smallest multichannel coil combination that covered the whole abdomen and pelvis.

Tumours were initially identified using conventional imaging sequences: (1) coronal and axial two-dimensional dual-echo (TE,  $<10 \text{ ms}$  and  $>50 \text{ ms}$ ) short-tau inversion recovery (STIR) spin-echo (TI/TR, 130 ms/ $>4,000 \text{ ms}$ ) with prospective diaphragmatic gating; (2) axial T2-weighted fast spin-echo (TR/TE,  $>2,500 \text{ ms}/50\text{--}70 \text{ ms}$ ) with prospective diaphragmatic gating.

Diffusion-sensitised 2-D single-shot spin-echo imaging was performed in the axial plane during free breathing. This was planned using the conventional sequences by centering the acquisition slab on the tumour and using up to 19 sections to cover the entire tumour with section thickness, 6 mm; intersection gap, 1.2–2.4 mm, TR/TE, 2,600 ms/89 ms; field of view, 350 mm with a rectangular factor of 75%; echo-planar readout with matrix of 128 and 96 phase-encoding steps; receive bandwidth, 1,500 Hz/pixel; parallel imaging factor, 2. We used signal averaging of six acquisitions and diffusion-sensitising gradients in three orthogonal planes with b values of 0, 50, 100, 250, 500, 750 and  $1,000 \text{ s/mm}^2$ . ADC was calculated from the b 0 images and from the averaged b 1,000 images. The acquisitions performed at lower b values were performed in case signal-to-noise at b 1,000 was insufficient for reliable calculations. Fat signal was suppressed using a frequency-selective radio-frequency preparation pulse. Total acquisition time for this sequence was 5.3 min. Diffusion-weighted images were always acquired before administration of gadolinium-based contrast material.

Fat-suppressed T1-W images were obtained before and after intravenous administration of gadolinium-based contrast. This was either a fast 2-D spin-echo sequence (TR/TE, 450–550 ms/8–18 ms) with a selective water-exciting radio-frequency pulse, acquired during free-breathing, which was the preferred sequence for anaesthetised children; or a fast low-angle shot 2-D gradient-echo sequence (TR/TE/flip angle, 1,500 ms/7 ms/ $15^\circ$ ) with a selective water-exciting radio-frequency pulse and prospective diaphragmatic gating that was used as a faster alternative in awake or moderately sedated children.

### Image analysis

Image analysis for each child, tumour and imaging episode was performed by two paediatric radiologists in consensus (K.M. and Ø.E.O.; 2 years and 7 years of experience with paediatric abdominal MRI, respectively). Masking was not attempted since it was usually obvious whether images had been acquired before or after chemotherapy.

The MR scanner software (Syngo, Siemens, Erlangen, Germany) calculated ADC maps by pixel-wise averaging the signal intensity in three orthogonal planes for each b value and subsequently calculating the slope of the

logarithmic decay curve for signal intensity against  $b$  value.

From the ADC maps we extracted the pixels contained within tumours using the DICOM software Osirix (available free online at <http://www.osirix-viewer.com>) version 3. This was achieved by drawing a region-of-interest (ROI) around the perimeter of tumour at each section. Perilesional oedema was not included in the ROIs. To reduce the effect of partial voluming, only sections at which tumour area was 3 cm<sup>2</sup> or more were included. Conventional MR images were used to guide tracing of the tumour outline.

Since we were only interested in the viable portions of tumours, we performed an exclusion of internal areas of assumed necrosis or low viability. For this we used the pre-contrast and contrast-enhanced T1-W images. In Osirix we subtracted the pre-gadolinium from the post-gadolinium T1-W images. Further processing was done in the image analysis suite ImageJ (Research Service Branch, National Institute of Health, Bethesda, MD, USA; available free online at <http://rsb.info.nih.gov/ij>) version 1.4. We thresholded the subtracted set so that only pixels with an enhancement at or above that of the erector spinae muscles were included. This was then used as a threshold filter for the ADC data set. The resulting filtered ADC data set therefore represented all pixels from all enhancing parts of tumour. The difference in voxel size between the T1 and ADC data sets was not an obstacle to this approach, since the ADC maps always had the lower spatial resolution. The individual pixel values were then exported in a comma-separated data format for statistical analysis.

### Histopathology

Histological slices from the surgically resected tumours were reviewed and reported according to current practice for assessment of chemotherapy response by one consultant paediatric histopathologist (N.J.S.; more than 10 years of experience with paediatric tumour histopathology), who was masked to the MRI findings.

### Statistical analysis

SPSS version 16 for Mac (SPSS Inc., Chicago, IL, USA) was used for all statistical analyses. Due to the small number of cases, the variety of diagnoses and response patterns, and since the aim of the paper was explorative, no comparative analysis was done. For each patient and scan event, the distribution of ADC values from all pixels within the volume-of-interest was tested for normality using the Kolmogorov-Smirnov test with the Lilliefors significance correction. Since all ADC distributions except one deviated from a normal distribution, the median was chosen to

represent the central tendency of a distribution. For each tumour and imaging episode we plotted the log-transformed relative frequencies of ADC in a histogram with bin widths of  $0.05 \times 10^{-3}$  mm<sup>2</sup>/s.

### Results

Lesion identifiers and details of all cases, diagnoses, median ADC, tumour volume change and histopathological chemotherapy response are listed in Table 1. Examples of conventional imaging, ADC maps and ADC distribution histograms before and after chemotherapy are demonstrated in Fig. 1 (lesion 3-b) and Fig. 2 (lesion 5-b).

Seven children (four girls) with a total of nine solid abdominal tumours (six nephroblastomas, two pelvic rhabdomyosarcomas, one hepatoblastoma) were included. Median age at primary diagnosis was 303 d (range, 248 d to 3 years 3 months). The interval between the pre- and post-chemotherapy scans was median 69 d (range, 32–110 d). One child (patient 1) with hepatoblastoma had an additional scan 48 d after the first scan. In patients 1–5, surgical resection of the tumour was carried out at a maximum of 10 d following the last scan. In patients 7 and 8, both with pelvic rhabdomyosarcoma, the delay was 76 d and 67 d, respectively.

All ADC distributions deviated significantly from statistically normal distribution ( $P < 0.001$ ), except for patient 6, after chemotherapy. ADC distributions for all lesions and scans are shown in Fig. 3.

Change in ADC distribution following chemotherapy was observed in every child. Median ADC increased in patients 1–5. The largest absolute increase ( $0.14 \times 10^{-3}$  mm<sup>2</sup>/s or more) was seen in tumours that histopathologically showed good or marked chemotherapy response (patients 1 and 2) or predominantly stromal differentiation following chemotherapy (patients 3 and 4). In patients 1–4 there was also a clear alteration of the shape of the distribution curve with a wider range of ADC values after chemotherapy. Despite showing a marked histopathological response in terms of identifiable chemotherapy-induced changes, the tumour of patient 4 more than doubled in volume during chemotherapy. Only a very small absolute increase ( $0.08 \times 10^{-3}$  mm<sup>2</sup>/s or less) and a narrowing of the ADC distribution curve was seen in two lesions (patient 5, bilateral nephroblastoma) that histopathologically were composed of 95% viable tumour following chemotherapy, and this was despite a marked volume reduction of 62% and 83%, respectively.

Two pelvic rhabdomyosarcomas (patients 6 and 7) were difficult to measure after treatment due to a marked volume decrease (92% and 95%, respectively) and due to their location deep within the pelvis. Both showed higher ADC values at the time of diagnosis ( $1.79 \times 10^{-3}$  mm<sup>2</sup>/s

**Table 1** Details of lesion identifier, diagnosis, scan intervals, median ADC before and after chemotherapy, ADC and volume change and histopathological review findings

Lesion ID Sex/ age at diagnosis (d)	Diagnosis	Scan interval (d) <sup>a</sup>	Pre-surgery scan interval (d) <sup>b</sup>	Median ADC, $\times 10^{-3} \text{mm}^2/\text{s}$		Volume change during chemo- therapy	Surgical specimen, histopathological findings	Histopathological chemotherapy- induced response
				At diagnosis	After chemo- therapy			
1 M/313	Hepatoblastoma	105	10	0.94	2.17	1.23	Fibrous replacement of tumour and conversion of cellular embryonal elements to more mature less cellular foetal elements (maturation)	Good
2 M/261	Nephroblastoma	32	7	1.16	1.97	0.81	50% necrotic In viable part: <5% blastema, 40% tubules, remainder stroma with rhabdomyomatous differentiation	Marked
3-a F/248	Nephroblastoma	110	9	1.00	1.78	0.78	<10% necrosis, 75% stroma with rhabdomyoblasts, some tubules, no blastema	Minimal
3-b F/248	Nephroblastoma	110	9	0.99	1.40	0.41	<10% necrosis, 75% stroma with rhabdomyoblasts, some tubules, <10% blastema	Minimal
4 F/683	Nephroblastoma	69	3	1.22	1.36	0.14	>95% viable, >90% stromal with rhabdomyomatous differentiation, <5% cellular blastema	Minimal
5-a M/303	Nephroblastoma	67	6	0.70	0.73	0.03	95% viable, >90% epithelial tubules	Minimal
5-b M/303	Nephroblastoma	67	6	0.79	0.87	0.08	95% viable, >90% epithelial tubules	Minimal
6 F/290	Bladder rhabdomyosarcoma	76	52	1.79	1.65	-0.14	Oedema, hyalinisation and only scattered differentiated rhabdomyoblasts.	Good
7 F/1,180	Pelvic rhabdomyosarcoma	67	36	1.53	1.21	-0.32	Generally loose stromal tumour, mainly viable with variably cellular areas—spindled, differentiating and cellular	Good

<sup>a</sup> Interval between the MRI at diagnosis before start of chemotherapy and the MRI before surgical resection after chemotherapy<sup>b</sup> Interval between the post-chemotherapy MRI and surgical resection

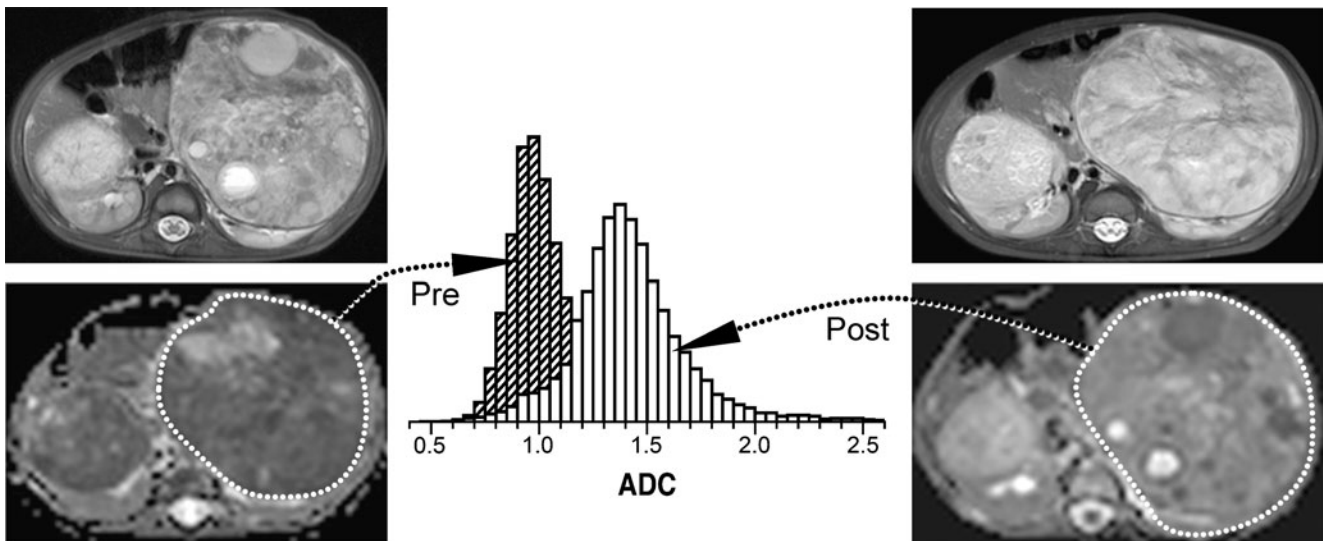


**Fig. 1** MRI and ADC histogram of an infant girl with bilateral nephroblastoma (lesion 3-b in Table 1). Images on the left are from the time of diagnosis (age, 248 d) and on the right following chemotherapy (110 d later). Top images, axial STIR (TI/TR/TE, 130 ms/4,800 ms/130 ms). Bottom images, axial ADC maps calculated from diffusion-sensitised acquisitions (b values, 0, 50, 100, 250, 500, 750 and 1,000 s/mm<sup>2</sup>). The histograms represent frequencies (y-axis, linear scale) of pixels with ADC-values ( $\times 10^{-3}$  mm<sup>2</sup>/s) given along the x-axis in bins of 0.05. At the time of diagnosis (*bars with diagonal*

*lines*), median ADC was  $0.99 \times 10^{-3}$  mm<sup>2</sup>/s and after chemotherapy (*white bars*) it increased to  $1.40 \times 10^{-3}$  mm<sup>2</sup>/s with a wider range of ADC-values. The higher ADC is reflected in the ADC map (*bottom right*), which is brighter than the corresponding map before treatment (*bottom left*). However, there was no difference in size as can be seen by the identical areas under the distribution curves. Histopathologically there was some chemotherapy response with predominantly stromal elements and rhabdomyomatous differentiation following chemotherapy

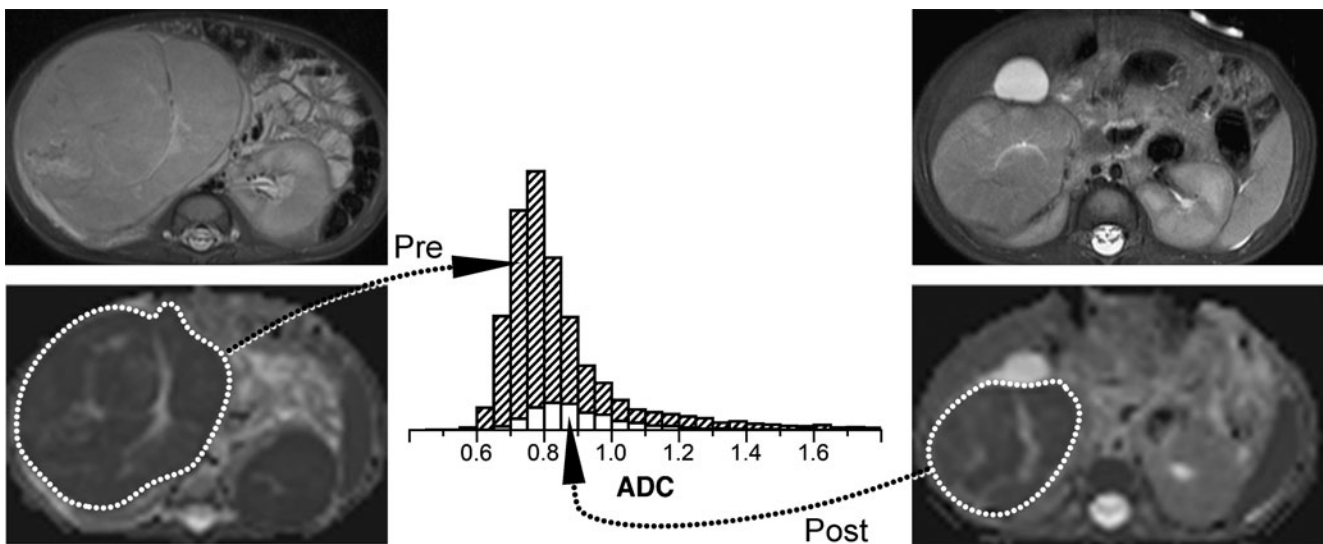
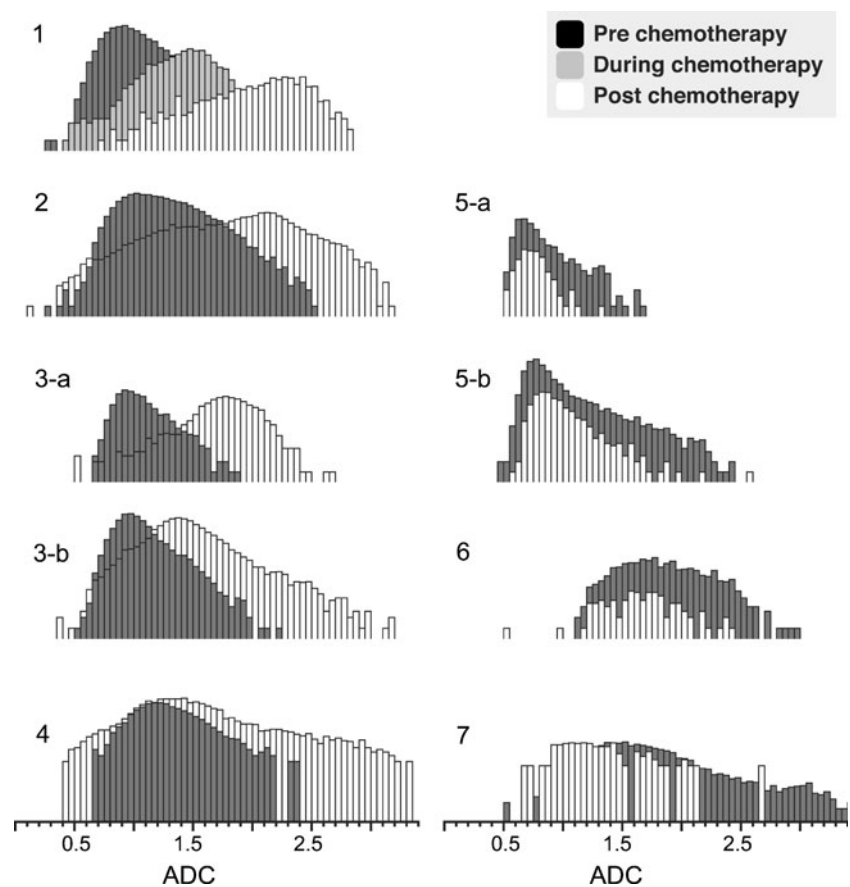


**Fig. 2** MRI and histogram of ADC values of an infant boy with bilateral nephroblastoma (lesion 5-b in Table 1). Images on the left are from the time of diagnosis (age, 303 d) and on the right following chemotherapy (67 d later). Top images, axial STIR spin-echo (TI/TR/TE, 130 ms/4,800 ms/130 ms). Bottom images, axial ADC maps calculated from diffusion-sensitised acquisitions (b values, 0, 50, 100, 250, 500, 750 and 1,000 s/mm<sup>2</sup>). The histograms represent frequencies (y-axis, linear scale) of pixels with ADC-values ( $\times 10^{-3}$  mm<sup>2</sup>/s)

given along the x-axis in bins of 0.05. At the time of diagnosis (*bars with diagonal lines*), median ADC was  $0.79 \times 10^{-3}$  mm<sup>2</sup>/s and after chemotherapy (*white bars*) it increased only slightly to  $0.87 \times 10^{-3}$  mm<sup>2</sup>/s with a narrower range of ADC-values. Shrinkage is evident in the smaller area under the distribution curve seen after chemotherapy. Volume change was  $-83\%$ . Histopathologically there was little chemotherapy change and high viability with predominantly epithelial tubules

**Fig. 3** Distribution of ADC in entire lesions excluding non-viable parts, before and after chemotherapy. An additional intermediate scan was done in lesion 1. Lesion numbering refers to Table 1. ADC-values ( $\times 10^{-3}$  mm<sup>2</sup>/s) in bins of 0.05 are plotted along the x-axis and the frequency of pixels per bin along the y-axis (log-scale). Median ADC and volume change are given in Table 1



and  $1.53 \times 10^{-3}$  mm<sup>2</sup>/s, respectively) compared to the lower ADC of the upper abdominal tumours (median,  $0.99 \times 10^{-3}$  mm<sup>2</sup>/s; range  $0.70 \times 10^{-3}$ – $1.22 \times 10^{-3}$  mm<sup>2</sup>/s). These pelvic tumours demonstrated a decrease in ADC following chemotherapy ( $-0.14 \times 10^{-3}$  mm<sup>2</sup>/s and  $-0.32 \times 10^{-3}$  mm<sup>2</sup>/s, respectively), despite showing good histopathological response.

## Discussion

A difference in the distribution of ADC values before and after chemotherapy was seen in all lesions in our study. This demonstrates the feasibility of the method. It does not, however, prove any causality since we did not include a control group. Nor does it prove any specific relation between the pattern of ADC shift and actual treatment response; more homogeneous diagnostic groups and larger numbers of patients would be required for such a study. Since this was a feasibility study with a small number of observations, formal statistical evaluation of patterns of change could not be done; the presentation of the results is therefore purely descriptive. For the same reason, it would be wrong at this early stage to suggest any specific cut-off values for clinical evaluation of treatment response.

Three technical observations can be made. (1) It is feasible to represent the ADC of the entire population of voxels within a tumour. This practice should be encouraged because tumours are often histopathologically heterogeneous and subregions within a tumour may respond differently to treatment. Care should be taken to avoid including any surrounding tissue oedema in the volume-of-interest, as this would add high-ADC voxels to the distribution. For this reason we used conventional images as a guide when drawing ROIs as close to the outline of tumour as possible and we did not include the extreme superior/inferior slices where partial voluming of extratumoral tissues might skew the ADC distribution. (2) The importance of excluding necrotic elements has been emphasised in previous studies [5]. It is feasible to exclude presumed nonviable portions of tumour from ADC analysis by applying a thresholding filter based on the degree of tissue enhancement following intravenous gadolinium administration. Our method of using the back muscles as a thresholding reference may seem arbitrary and this could have been improved by using formal perfusion analysis. Theoretically it is valuable to attempt such tissue separation because ADC values of necrotic areas, in our experience, can sometimes be so low that they mimic highly cellular portions of tumour. An additional rationale for this

approach is that quantitative techniques, such as ADC analysis, should be used to provide new information that would not be available with conventional techniques. Since conventional MR sequences combined with enhancement information already provide the facility to distinguish viable from necrotic tissue, such separation should take place so that ADC is analysed, as far as practically possible, only in viable regions. (3) The ADC distributions in our study did not conform to a statistically normal distribution. The distribution histograms showed a mixture of right and left shoulders and we also observed differences in the width of the distributions before and after chemotherapy. These observations should caution against using only a central value to represent the whole population of voxels since the overall shape of the distribution curve may in itself be a biological marker. Theoretically, for example, a substantial left shoulder may indicate a large sub-population of highly cellular, malignant tissue. Conversely, a marked right shoulder may indicate substantial oedematous or cystic portions. Assessment of the distribution curve for such skewness is therefore recommended. However, when a single value representation is practical, for example when comparing two or more distributions, we recommend using the median.

Although our study did not intend to prove a specific relation between ADC change and histopathological response, some speculations can be made. (1) We observed moderate ( $\geq 0.14 \times 10^{-3} \text{ mm}^2/\text{s}$ ) or marked absolute increases in median ADC in those upper abdominal tumours that histopathologically demonstrated either good or marked chemotherapy-induced change or that showed predominantly stromal elements with prominent rhabdomyomatous differentiation after chemotherapy. This corresponds well with the findings in a previous study of bone sarcomas; however, direct comparison is difficult [6]. These responding tumours also showed a wider ADC distribution following chemotherapy with a relatively large proportion of voxels exceeding the upper limit of the ADC distribution seen before chemotherapy. It may be hypothesised from this that the observed right-shift in ADC was caused by decreasing tumour cellularity in response to chemotherapy, a thought that is underpinned by the known relation between increasing tissue cellularity and decreasing ADC [3]. (2) Two lesions that histopathologically showed minimal response and were almost entirely viable, non-stromal following chemotherapy (lesions 5-a and 5-b), demonstrated a different pattern of ADC change with a clear narrowing of the ADC distribution and only a minimal ( $\leq 0.08 \times 10^{-3} \text{ mm}^2/\text{s}$ ) absolute increase in median ADC. It is possible that this unique pattern of ADC change reflects unchanged tumour cellularity. This may in itself be interesting as a possible expression of poor chemotherapy response, although it may have little relevance in terms of current histopathological risk classification,

which in the case of nephroblastoma only recognises anaplasia and diffuse blastema, and not non-response *per se*, as markers of high risk [7]. (3) The two pelvic rhabdomyosarcomas in our study did not appear to follow any of the patterns demonstrated with the other malignancies. These cases were characterised by a high ADC at the time of diagnosis, and very small post-chemotherapy volumes that were difficult to distinguish from surrounding tissue. Any of these characteristics (rhabdomyosarcoma, deep pelvis location, high ADC at the time of diagnosis, small post treatment volume) may therefore discourage therapy assessment by ADC, but we cannot draw any firm conclusions. An alternative explanation is that the interval between the post-chemotherapy scan and surgical resection was particularly long in these patients (76 d and 67 d, respectively; compared to maximum 10 d in the remaining patients), and it is conceivable that this has introduced discrepancy.

Two cases demonstrated discordance between volume change and chemotherapy response. One tumour (patient 4, nephroblastoma) more than doubled in size during chemotherapy, but demonstrated rhabdomyomatous differentiation and predominantly stromal elements after treatment. Whereas by size criteria this would be classified as progressive disease, median ADC increased and the ADC distribution widened during treatment, which fits the theoretical pattern for treatment response. The opposite was seen in two lesions (patient 5, bilateral nephroblastoma). These tumours decreased in size during chemotherapy, but on histopathological assessment there was very little suggestion of chemotherapy-induced changes, and both were almost entirely viable. Whereas by size criteria these lesions responded to treatment, the ADC shifts (narrowing of the distribution and almost no change in median ADC) were distinctly different from the response pattern. It is well-documented that volume change does not necessarily predict biological response in paediatric tumours [2, 8], as was the case in these two children. Volume increase may be caused by internal haemorrhage and an enlarging tumour may contain large necrotic areas. When this is the case, even US, CT and conventional MR techniques would be able to differentiate. In solid, viable tumours, however, new methods are needed for detecting likely histopathological non-response in a shrinking tumour and response in a growing tumour. Our finding that ADC change is independent of volume change is therefore promising, and should encourage further studies of the relation between changes in ADC distribution with chemotherapy and biological response.

Some limitations in ADC evaluation relate to the lack of standardisation of the technique, e.g., the choice of b values. Although this is not a problem in a single-centre study like ours, problems may arise in multicentre studies and in meta-analyses. Future studies therefore ought to observe particular prudence if suggesting a specific absolute ADC change as cut-off value in therapy assessment.

## Conclusion

Shifts in ADC distribution in viable parts of childhood abdominal tumours are common and measurable. Several distinct patterns of shift can be observed and the technique is therefore promising as a noninvasive biomarker for therapy response. Our data suggest that upper abdominal tumours and renal tumours in particular, may be the best candidates for future studies.

## References

1. Gow KW, Roberts IF, Jamieson DH et al (2000) Local staging of Wilms' tumor—computerized tomography correlation with histological findings. *J Pediatr Surg* 35:677–679
2. Olsen ØE, Jeanes AC, Sebire NJ et al (2004) Changes in computed tomography features following preoperative chemotherapy for nephroblastoma: relation to histopathological classification. *Eur Radiol* 14:990–994
3. Humphries PD, Sebire NJ, Siegel MJ et al (2007) Tumors in pediatric patients at diffusion-weighted MR imaging: apparent diffusion coefficient and tumor cellularity. *Radiology* 245:848–854
4. Sury MR, Smith JH (2008) Deep sedation and minimal anesthesia. *Paediatr Anaesth* 18:18–24
5. Pickles MD, Gibbs P, Lowry M et al (2006) Diffusion changes precede size reduction in neoadjuvant treatment of breast cancer. *Magn Reson Imaging* 24:843–847
6. Uhl M, Saueressig U, Koehler G et al (2006) Evaluation of tumour necrosis during chemotherapy with diffusion-weighted MR imaging: preliminary results in osteosarcomas. *Pediatr Radiol* 36:1306–1311
7. Vujanic GM, Sandstedt B, Harms D et al (2002) Revised International Society of Paediatric Oncology (SIOP) working classification of renal tumors of childhood. *Med Pediatr Oncol* 38:79–82
8. Anderson J, Slater O, McHugh K et al (2002) Response without shrinkage in bilateral Wilms tumor: significance of rhabdomyomatous histology. *J Pediatr Hematol Oncol* 24:31–34